Georg Schober

Ingenieurbüro für Material- und Verfahrenstechnik, Sägmühlstraße 14, 82140 Olching, Germany

Porosity in autoclaved aerated concrete (AAC): A review on pore structure, types of porosity, measurement methods and effects of porosity on properties

ABSTRACT: The fraction of pore volume in AAC products covers the range from 65 to 90%. There is a set of different types of pores, e.g. large air pores are a macroscopic structural element, capillary pores and nano pores, which are connected to microstructure of the solid matrix and have specific functional effects. Different methods of pore generation and characterization of pore size distribution are summarized. Gas producing agents, foaming agents, prefabricated foam and voluminous water retarding components are compared with regard on their suitability for AAC product properties. Image analysis, mercury intrusion porosimetry, gas adsorption porosimetry and other methods are reviewed with respect of their application for AAC material. Influence of pore size, pore shape, proportion of different pore types on related properties is presented and discussed. Homogeneity of material, isotropy of properties and range of property values with respect to porosity influences are regarded.

KEY WORDS: AAC, air pores, microstructure, pore size distribution, porosity

1. Pore types in autoclaved aerated concrete

In AAC there are at least two types of pores which are often referred to as “macropores” and “micropores” in the business environment of AAC producers. The term macro pore is used for the large air pores, which are generated artificially by using a foaming agent or a foam. When talking about micropores all the porosity which is incorporated in the skeletal material around the air pores is generally meant.

Unfortunately the terms macro pore and micro pore are used differently in the scientific field. In most research works this two kinds of pores are clearly defined. Macropores are pores with diameters more than 50 nm and micropores have pore sizes lower than 2 nm in pore diameters. The gap between these two ranges is covered by the so called meso pores. These definitions are common in porosimetry when adsorption methods were applied.

To avoid misinterpretations in this paper the terms “macropore” and “micropore” will not be used as trivial names for the two types of pores as common in the AAC industry. The large pores will be named “air pores” and the latter will be referred to as “pores in the skeletal material”.

1.1. The air pores in AAC

The most evident pores in AAC are the artificial air pores of millimetre size. These large pores make up the characteristic surface of AAC material when it is broken or cut by saw in its finished state. Masonry units of AAC and most of the AAC products normally don’t show the real air pore structure on their surfaces. The units are cut by means of wires during processing after procuring that produces specific surface structures that cover the air pore structure more or less.

The shape of air pores in most cases is nearly spherical. As AAC products are produced in a wide range of density classes, 300 to 800 kg/m^3, and these variations are mainly induced by changing the number of artificial air pores, the pore distances of air pores in AAC may range from one millimetre down to zero which means the pores are touching each other or are even interconnected [13, 7]. In the cases of low density classes, when there are large numbers of air pores which touch each other, some deformation of the spheres is present due to these contacts. There is no evidence neither in industrial AAC products nor in lab made AAC samples that the air pores are generally elliptical in shape, e.g. regularly flattened pores, as was assumed by Cabrillac [2].

The sizes of air pores in AAC are always in the millimetre size range, most of them have diameters between 0.5 to 3.0 mm. The

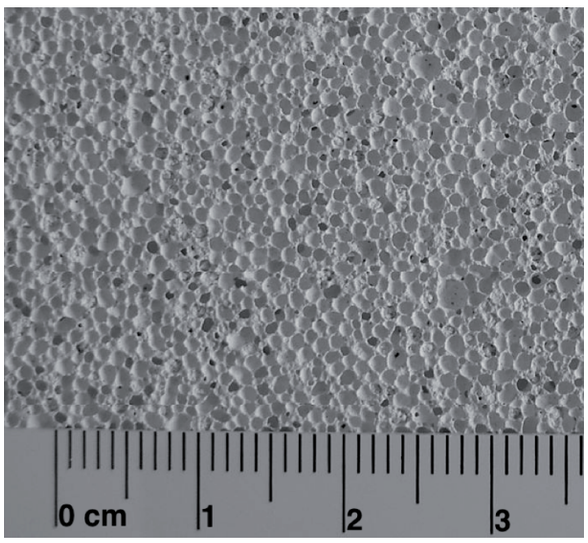

Fig. 1. Air pore structure of an AAC sample.

size distribution of air pores in AAC is generally a mono modal and narrow one [12, 15]. It is primarily a matter of porosing agent or method which medium size of air pores will be generated. The air pores introduced in AAC during manufacturing process are contributing between 25 to 70% to the total pore volume which ranges from 65 to 90%.

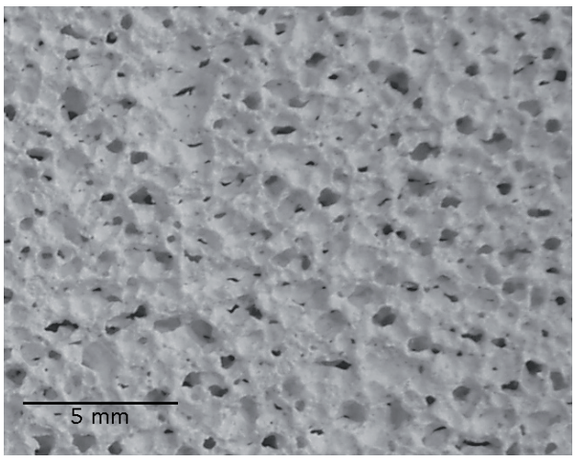

Fig. 2. Air pores and expanding crack structure of an AAC sample made with aluminium powder as expanding agent.

The expanding crack structure is a substantial pore structure element in AAC material made with aluminium. The cracks own a preferred orientation, they lie horizontal when rising direction is upward. Most of them are interconnecting the air pores [16]. Thus AAC has an open cell structure with regard to air pores. Only high-density material of AAC, more than 550 kg/m^3, can possess pore distances as large as a closed cell structure of air pores may be formed.

1.2. The pores in the skeletal material

The porosity in the matrix material, the skeleton around the air pores in AAC, is composed of different types of pores. There is the space, which was originally filled with water and partly has become occupied by reaction products during pre-curing and autoclaving, Fig. 3. Then there is some volume, which at first was taken by quartz grains that is partly or completely turned to pore volume as quartz was dissolved during autoclaving, Fig. 3 and 4. And finally all the reaction products, mainly tobermorite, produced new pore space between the newly formed crystals. These inter particle pores correspond in their sizes to the size of crystals formed. One example is shown in Fig. 5 the large platelet tobermorite crystals. But the major part of matrix material is composed of very tiny tobermorite and C-S-H crystals and the corresponding pore size is of nm scale.

A part of the open space shown in Fig. 3 originally has been occupied by a quartz grain, which has been dissolved during hydrothermal processing almost completely. Another part of the open space may have been occupied by water.

The dissolution of quartz during autoclaving process can produce residual quartz of the kind shown in Fig. 4. The residual quartz

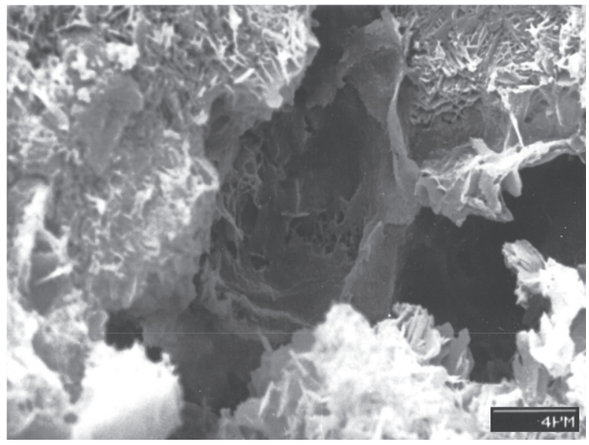

Fig. 3. Hollow spaces in the skeleton material of AAC. In the centre of the picture there is a small residue of quartz.

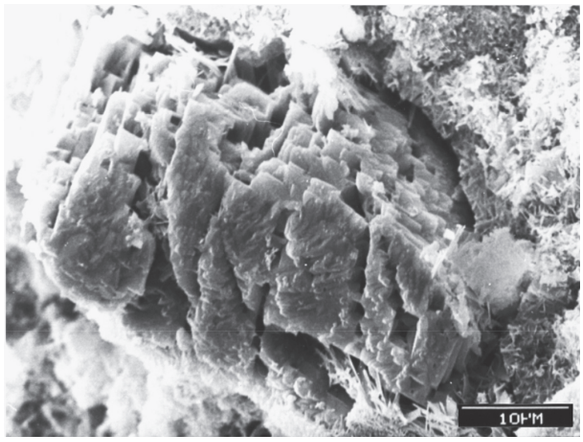

Fig. 4. A quartz grain with interior pores surrounded by tobermorite material in AAC.

in AAC is not generally in a state like this. Some of compact residual quartz grains in AAC often are not built in densely into the microstructure. Quartz, which was not completely dissolved during autoclaving, may rest in holes with a gap of free space around inside the matrix of tobermorite. In Fig. 4 at the right upper rim of the grain such a gap is depicted.

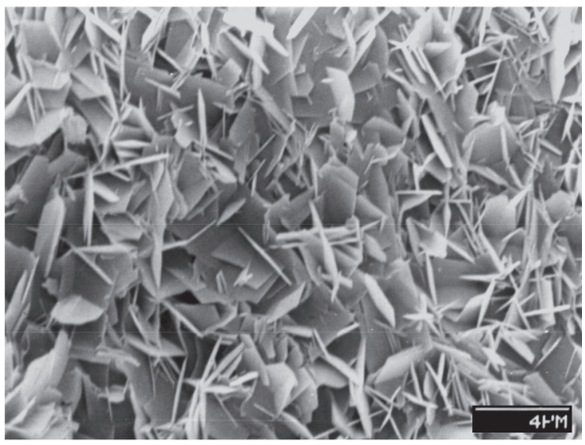

Fig. 5. The tobermorite material in AAC as it is found on the pore walls inside air pores.

The coarsest kind of tobermorite crystals present in AAC is visible in Fig. 5, connected to these crystals is porosity, which is defined by size and shape of tobermorite particles.

Similar to the situation with large tobermorite crystals, the main volume of binding material in AAC, which consists of tobermorite or calcium-silicate-hydrate (C-S-H) phases of very low crystallite sizes, possesses porosity conjoined to these crystallites.

Table 1. Classification of porosity in AAC material.

	Size range, diameter/ µm	Description	Trivial names
	100 - 3000	Artificial gas pores generated by hydrogen from aluminium reaction (in some cases foam pores) with expanding crack structure	Air pores, Gas pores, "macro pores"
	5 - 30	Residual pore space of initially water filled volume	Water pores, Inter cluster pores, "micro pores"
	10 - 50	Holes as residuals of dissolved quartz particles, Hollows around residual quartz grains	Quartz grain related pores, "micro pores"
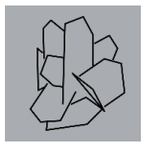	0.5 - 20	Pore volume between new formed large crystals of tobermorite	Inter particle pores, Tobermorite related pores, "micro pores"
?	0.005 - 1	Pore volume between new formed crystallites of tobermorite and CSH phases	Nano pores, CSH phases related pores, "micro pores"

1.3. Summary on types of pores in AAC

The pore volume in AAC is mainly constituted of air pores and nano pores, see Fig. 6, where a complete pore size distribution is illustrated.

2. Methods of pore generation

The porosity in AAC for a certain part is produced with intends to achieve the appropiate density class for the product. The standard procedure in AAC production to adjust density is to use aluminium powder as gas generating agent and dose the aluminium in the appropriate amount. Aluminium generates hydrogen in the mixture of raw materials in form of gas bubbles [1].

Alternative ways to generate high porosity are using foaming agents or prefabricated foam. With the first method the raw materials slurry is mixed together with the foaming agent to get high porous foam slurries, the latter method requires carefully mixing the raw materials slurry with the prepared foam. A different technique to achieve high pore volumes is to use as much water as needed to have the wanted porosity, this requires water retarding agents or soaking materials as mixture components. And finally it is possible to add foaming agents or materials, which introduce pores in the nanoscale range (e.g. surfactants).

In AAC industry the method with aluminium is common since decades and has no serious competition. The use of water retarding agents would indicate a costly drying after autoclaving and working with foams produces a cake after pre-curing which behaves less controllable during steam curing. The introduction of additional nanoscale pores is only a research topic so far.

3. Porosimetry, pore size distribution

To determine total porosity of AAC it is necessary to measure true density of crushed material as some closed porosity exists. Kadashevich and Janz give some values for true density of AAC, which lay around 2,6 kg/m^3 [7, 6].

Methods to measure open pore volume like water saturation under vacuum or mercury intrusion porosimetry (MIP) can be employed to AAC materials [5, 11, 4]. The water saturation method is suitable to get the total open pore volume of AAC. MIP is physically restricted to a maximum size of detectable pores of around 1 mm in diameter, and most of the available equipments allow to measure up to 200 or 300 µm pores only. So the water saturation method under vacuum alone will provide correct values of total open porosity in AAC.

The MIP is preferred to determine the pore size distribution as it covers a wide range in pores sizes, from 5 nm till 1 mm. One has to keep in mind that most of the air pores in AAC cannot be detected by MIP, and that there are some restrictions as MIP results in wrong pore sizes for inkbottle pores and bottle neck pore structures, and parts of the pore structure may be destroyed during a measurement run with MIP. Nevertheless, most of the available pore size data for AAC are MIP data.

For detecting air pore sizes and size distribution light or scanning electron microscope in combination with image analysis (IA) is common [12, 15, 5, 7]. If sample preparation and image digitalization is managed with standard procedures quantitative IA is a reliable method.

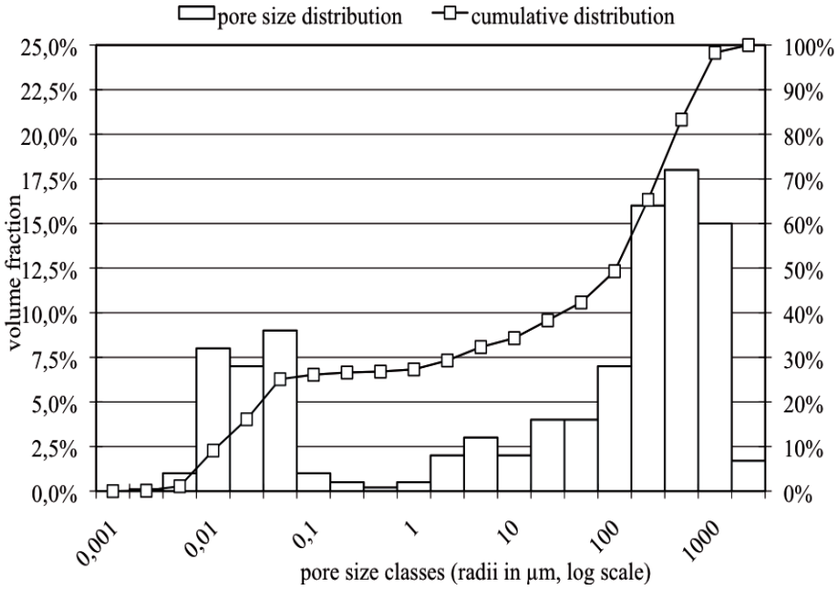

Fig. 6. Pore size distribution in an AAC sample from MIP and IA combined data.

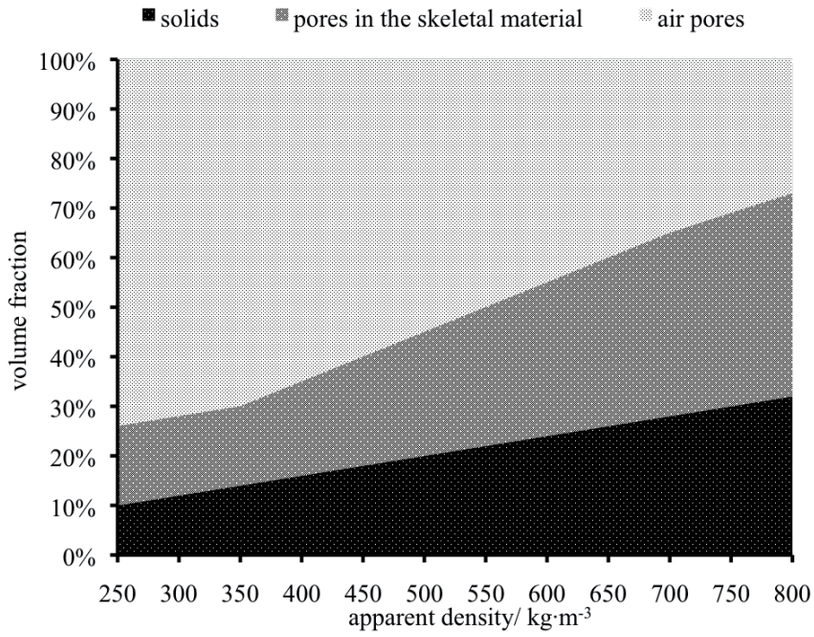

Fig. 7. The volume fractions in AAC of pore types and solids with different density.

The combination of MIP and IA leads to pore size distribution data covering the complete size range of pores in AAC [13, 17]. A typical result is shown in Fig. 6.

With X-ray computed tomography a 3D analysis of pore structures is available [10, 9]. For AAC this method is used too but no published data are available so far. The X-ray micro-computed tomography resolves structures of µm size.

For the low size range of pores gas absorption (nitrogen or water vapour) methods may be used. With absorption the pore size range below 50 nm can be evaluated. For AAC material mainly BET specific surface data are reported. The adsorption methods are preferred to investigate fluids transport properties, a pore size interpretation is rarely given in most of these works [17, 19, 8].

4. Properties influenced by porosity

4.1. Strength

As density is connected to porosity the different density classes of AAC ought to have different strength properties. The relation between porosity and strength with AAC is known to be exponential [15, 14, 16]. The alteration of pore volume with respect to densities primarily concerns the air pores, so the changes in strength with porosity are first of all an effect of air pore volume. The size of air pores has no notable influence on strength [15, 16]. The expansion crack structure is responsible for the anisotropy in strength [16].

4.2. Thermal conductivity

Porosity and thermal conductivity are inversely proportional in the range of ordinary AAC density classes [18]. Improvement of thermal insulation basically needs increase if porosity. But building materials like AAC are never completely dry when in use, thus the pores which are filled with moisture and their properties determine the thermal behaviour for insulation purpose too [3]. All measures which change the amount and the state of nano pores may influence the thermal properties of AAC by indirect effects (equilibrium moisture content, moisture transport, heat transfer by radiation).

4.3. Transport phenomena to liquids and gases

Permeability to fluids is a basic effect which is controlled by porosity. In AAC the air pores and the expansion crack structure determines the permeability to gases [20]. For moisture and liquids transport the conditions reveal to be more complex. Depending on degree of saturation and interaction of pores and liquids the transport characteristic are varying within a wide range [6, 17].

5. Conclusion

AAC with its multi-hierarchical pore structure, which defines essential properties of AAC, relatively high strength and low thermal conductivity, is extraordinary in some aspects, the pore sizes vary from nm to mm scale and the most relevant size ranges lie at the lower and upper end of the distribution.

Efforts to reduce or even avoid anisotropy of strength, to lower the equilibrium moisture content and to establish gas filled nano pores may result in further improvement of materials properties.

References

[1] Aono Y. et al., 2005. Mechanisms and countermeasures against cavity defectives in AAC during manufacturing. Autoclaved Aerated Concrete - Innovation and Development, Taylor & Francis Group, London, pp. 39-48.

[2] Cabrillac R. et al. 2006, Experimental study of the mechanical anisotropy of aerated concretes and of the adjustment parameters of the introduced porosity. Construct. Build. Mater. **20 (5)**, 286-295.

[3] Gawin D.J. et al., 2004. Thermal Conductivity of Moist Cellular Concrete - Experimental and Numerical Study. ASHRAE Thermal IX Conference, pp. 1-10.

[4] Isu N. et al., 2005. Mechanical Property Evolution during Autoclaving Process of Aerated Concrete Using Slag: II, Fracture Toughness and Microstructure. J. Am. Ceram. Soc. **77 (8)**, 2093-2096.

[5] Jacobs F., Mayer G., 1992. Porosity and permeability of autoclaved aerated concrete. Advan. in AAC, 3rd RILEM Intern. Symposium on AAC, Balkema, Rotterdam, pp. 71-75.

[6] Janz M., 2002. Moisture diffusivities evaluated at high moisture levels from a series of water absorption tests. Mater. Struct. **35 (3)**, 141-148.

[7] Kadashevich I. et al., 2005. Statistical modeling of the geometrical structure of the system of artificial air pores in autoclaved aerated concrete. Cem. Concr. Res. **35 (8)**, 1495-1502.

[8] Koronthályová O., 2011. Moisture storage capacity and microstructure of ceramic brick and autoclaved aerated concrete. Construct. Build. Mater. **25**, 879-885.

[9] Kunhanandan Nambiar E.K., Ramamurthy K., 2007. Air-void characterisation of foam concrete. Cem. Concr. Res. **37 (2)**, 221-230

[10] Maire E. et al., 2003. X-ray tomography applied to the characterization of cellular materials. Related finite element modeling problems. Compos. Sci. Tech. **63 (16)**, 2431-3443.

[11] Mitsuda T. et al., 1992. Influence of hydrothermal processing on the properties of autoclaved aerated concrete. Advan. in AAC, 3rd RILEM Intern. Symposium on AAC, Balkema, Rotterdam, pp. 11-18.

[12] Petrov I., Schlegel E., 1994. Application of automatic image analysis for the investigation of autoclaved aerated concrete structure. Cem. Concr. Res. **24 (5)**, 830-840.

[13] Prim P., Wittmann F.H., 1983. Structure and water absorption of aerated concrete, in: F.H. Wittmann (Ed.), Autoclaved Aerated Concrete, Moisture and Properties, Elsevier, Amsterdam, pp. 55-69.

[14] Schneider T. et al., 1999. Strength modeling of brittle materials with two- and three-dimensional pore structures. Comp. Mat. Sci. **16 (1-4)**, 98-103.

[15] Schober G., 1992. Effect of size distribution of air pores in AAC on compressive strength. Advan. in AAC, 3rd RILEM Intern. Symposium on AAC, Balkema, Rotterdam, pp. 77-80.

[16] Schober G., 2005. The most important aspects of microstructure influencing strength of AAC. Autoclaved Aerated Concrete - Innovation and Development, Taylor & Francis Group, London, pp. 145-153.

[17] Roels S. et al., 2002. Modelling unsaturated moisture transport in autoclaved aerated concrete: a microstructural approach. Proc. 6th Symp. on Build. Physics in the Nordic Countries. **Vol. 1**, 167-174.

[18] Tada S., 1986. Material design of aerated concrete - An optimum performance design. Mater. Struct. **19 (1)**, 21-26.

[19] Tada S., 1992. Pore structure and moisture characteristics of porous inorganic building materials. Advan. in AAC, 3rd RILEM Intern. Symposium on AAC, Balkema, Rotterdam, pp. 53-63.

[20] Wägner F. et al., 1995. Measurement of the gas permeability of autoclaved aerated concrete in conjunction with its physical properties. Cem. Concr. Res. **25 (8)**, 1621-1626.